land

MDPI

Article

Insight into Carbon Emissions in Economically Developed Regions Based on Land Use Transitions: A Case Study of the Yangtze River Delta, China

Yu Li, Yanjun Zhang * and Xiaoyan Li

College of Earth Sciences, Jilin University, Changchun 130061, China; yuli22@mails.jlu.edu.cn (Y.L.); lxyan@jlu.edu.cn (X.L.)

* Correspondence: yanjunzhang@jlu.edu.cn; Tel.: +86-15144162288

Abstract: This study focused on the land use (LU) structure and carbon emissions (CEs) in the Jiangsu, Zhejiang, Anhui, and Shanghai provinces of the Yangtze River Delta (YRD) in China from 2000 to 2020, using the STIRPAT model and scenario analysis (SA). We conducted an analysis of the influence exerted by relevant factors on land use carbon emissions (LUCEs) and made forecasts regarding the diverse development scenarios of CE trends, aiming to provide methodological guidance for validating the effectiveness of existing policies in reducing CEs and offer direction for achieving the peak CO_2 emissions target as soon as possible. It also constitutes a significant reference for the early realization of the peak CO_2 emissions target. The results indicated the following: (1) Between 2000 and 2020, CEs resulting from LU in the YRD rose from 2.70×10^8 t to 9.10×10^8 t, marking an increase of 243.77%. In 2020, the built-up area was the predominant contributor to CEs, representing 99.15% of the overall carbon sources, whereas forests served as the main carbon sink, comprising 92.37% of the total carbon sinks (CSs) for that year. (2) For each percent increase in the parameters considered in this study, the corresponding increases in LU CO_2 emissions were estimated to be: 1.932% (population), 0.241% (GDP per capita), −0.141% (energy intensity), 0.043% (consumption structure), 1.045% (industrial structure), and 0.975% (urbanization). (3) According to the existing policy framework and development plans, the YRD is expected to achieve peaking carbon dioxide emissions by 2030. If energy conservation and carbon reduction strategies are implemented, this peak could be achieved as early as 2025. However, if economic growth continues to depend primarily on fossil fuel consumption, the region may not hit its carbon peak until 2035. (4) The low-carbon scenario, which considers the needs of social progress alongside the intensity of carbon emission reductions, represents the most effective development strategy for reaching a carbon peak in LU within the YRD. Effectively managing population size and facilitating the upgrading of industrial structures are key strategies to hasten the achievement of peaking carbon dioxide emissions in the region.

Keywords: Yangtze River Delta; land use; carbon emissions; STIRPAT; scenario analysis

Citation: Li, Y.; Zhang, Y.; Li, X. Insight into Carbon Emissions in Economically Developed Regions Based on Land Use Transitions: A Case Study of the Yangtze River Delta, China. *Land* **2024**, *13*, 1968. https://doi.org/10.3390/land13111968

Academic Editors: Jianjun Zhang and Xuechao Wang

Received: 14 September 2024
Revised: 17 November 2024
Accepted: 19 November 2024
Published: 20 November 2024

1. Introduction

As the global economy rapidly develops, the influence exerted by humanity on the Earth's environment has been increasingly manifested. The issues of global warming resulting from greenhouse gas emissions and the rising frequency of extreme weather events are becoming more serious [1,2]. The Paris Agreement, established in 2015, aimed to restrict the rise in global average temperature to no more than 1.5 °C. However, the situation remains severe, and the continued release of greenhouse gasses will lead to further global warming. There are worrying signs that critical thresholds may already have been passed, making the Paris Agreement's targets difficult to achieve [3]. Approximately one-third of the current global warming is linked to non-CO_2 greenhouse gasses (NCGGs) like methane (CH_4); however, carbon dioxide remains the main factor driving global warming [4]. China accounts for one-third of global carbon emissions (CEs), making it the world's largest

carbon emitter [5]. Consequently, China's initiatives to lower CEs are crucial for controlling global emissions and improving the global environment.

Land serves as a natural medium for carbon sinks (CSs) within terrestrial ecosystems and is a social–economic spatial carrier of human-produced CEs. Land use (LU) change influences the natural and anthropogenic carbon flux processes carried out by various types of LU by changing the natural surface cover and the intensity of human activities [6]. It is one of the most direct and significant anthropogenic driving factors affecting the carbon cycle in terrestrial ecosystems [7,8].Therefore, this research centers on land use carbon emissions (LUCEs) as its primary point of analysis.

Since the 1990s, the topic of CEs generated by LU has progressively garnered greater interest among researchers globally. The mechanisms and accounting [9–13] as well as the analysis of influential factors [14–17] of LUCEs have been one of the key research directions. For instance, Zhang et al. assessed the carbon sources and sinks associated with LU in China between 1999 and 2014 by employing the carbon emission coefficient, utilizing data on LU and energy consumption. The findings indicate that built-up area was the primary contributor to CEs and forest was the main CS [13]. Hung et al. estimated 10-year CEs based on land cover change in the Vietnamese region from 2002 to 2012 relying on land cover classification results [12]. These studies analyzed the main components of LUCEs through different calculation methods and models, providing important references for the development of scientific management policies.

In recent years, research estimating CO_2 emissions has emerged as a prominent area of study both domestically and internationally. In China, models employed in this field of research are commonly referred to as carbon emission prediction models (CEPMs), and an overview of the field in the Chinese context is provided by Jin et al. [18]. Such models include the IPAT model [19,20], STIRPAT model [21–24], Gray model [25–27], ARIMA model [28,29], neural network model [30], Logistic model [31], and the environmental Kuznets model [32].

For instance, Ye et al. investigated how economic, energy, population and LU structure influence LUCEs in Zhejiang Province, and applied the STIRPAT model to simulate and forecast the future trend in LUCEs. The results show that under the current economic development scenario, Zhejiang Province will achieve peaking carbon dioxide emissions by 2030 [24]. Fang et al. explored the pathway to achieving peaking CO_2 emissions in 30 Chinese provinces by establishing an extended STIRPAT model, analyzing the key factors that affect CEs in each province and forecasting the time of CO_2 emissions' peak with scenario analyses (SAs) [21]. Malik et al. applied the ARIMA model to project carbon dioxide emissions in Pakistan through 2030, yielding results with high accuracy [29]. Huang et al. used LSTM to estimate China's CEs and found that CO_2 emissions per unit GDP were expected to decrease by 30% from 2015 to 2020 [30].

Although existing research has achieved many important results, there are two inadequacies. Firstly, current studies that estimate CEs in the Chinese context primarily focus on estimating the emissions from urban areas or energy sources. These investigations typically only account for CO_2 emissions resulting from fossil fuel use and electricity generation, neglecting the CO_2 released during LU change processes. In China, this growing field generally does not integrate LU change and the socioeconomic development process to holistically consider CEs. Therefore, there remains a notable gap in the research forecasting LUCEs, and the lack of integration of LU structure and energy use carbon emission forecast analysis. Moreover, this strand of research does not allow decision-makers to verify whether peak CO_2 emissions and carbon neutrality goals can be achieved on time under existing policies.

Therefore, in order to have a more comprehensive understanding of the future trend of CEs under policy constraints and to assess the effectiveness of strategies aimed at social and economic development in reducing CEs, it is necessary to estimate the time of peak CO_2 emissions based on the calculation of LUCEs, combined with the social and economic development policies. As one of the most economically dynamic regions in

China, and featuring the highest intensity of energy consumption [33,34], the LU in the YRD is closely linked to social development, economic growth, industrial distribution, urban sprawl, and energy consumption. This study provides methodological guidance for validating the effectiveness of existing policies in reducing CEs for the government, provides direction for formulating effective carbon reduction policies for the government in different socioeconomic development scenarios in the future, and provides direction for achieving the peak CO_2 emissions target as soon as possible.

2. Materials and Methods

2.1. Study Area

The study area of this paper is situated in the YRD of China. (Figure 1). As per the "Development Plan Outline for the Integrated Development of the YRD", which was sanctioned by China's State Council in 2019, the YRD encompasses Jiangsu, Zhejiang, Anhui provinces, and Shanghai. This region consists of 41 cities and covers an area of 358,000 square kilometers. The study region is primarily composed of cropland, forest, and built-up area, which account for approximately 52%, 30%, and 12.5% of the total area, respectively. The YRD stands out as one of the most dynamic, accessible, and innovation-driven areas in China's economic growth. In 2022, the gross domestic product of the region amounted to 29.03 trillion yuan, which occupies a pivotal position in the national economy. However, the YRD is also one of the largest energy consumption and carbon emission regions in China [35]. Therefore, the study of LU and carbon emission in the YRD holds significant research value.

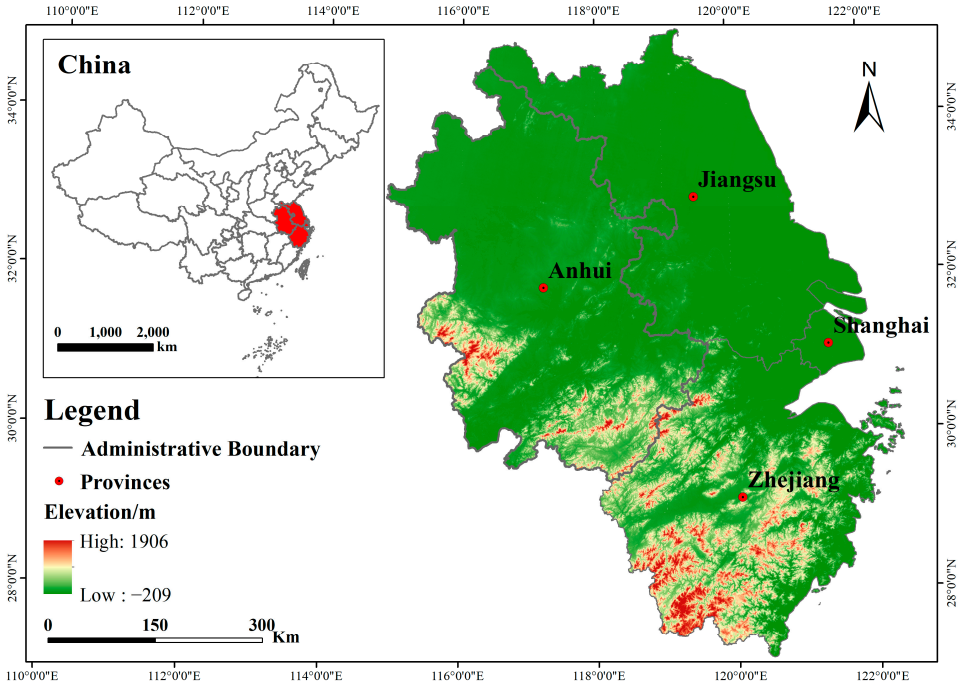

Figure 1. Schematic diagram of study area. (The data are derived from https://www.gscloud.cn/home, accessed on 25 October 2023).

2.2. Data Source

The data in this study mainly consists of three types (Table 1): LU data, socioeconomic development data, and energy consumption data. The LU data are derived from the 30 m land cover dataset developed by the research team of Yang Jie and Huang Xin from Wuhan University in China [36]. Using Landsat data, they achieved a continuous classification of LU for multiple years, with an overall classification accuracy of 80%. We selected 21 years of data from 2000 to 2020, and transformed the coordinate system of the remote sensing image into an Albers projection with the geographic coordinate system set to WGS1984. The LU

data includes six categories: built-up area, cropland, forest, grassland, water, and barren land. We used ArcGIS 10.6 to calculate the area of each LU type (see Section 3.1 below). This allowed us to calculate both changes over the twenty-year period in absolute terms, and the rates of change. The socioeconomic development data and energy consumption data were obtained from the statistical yearbooks for the period 2000–2020 for Shanghai, Zhejiang, Jiangsu, and Anhui, as well as the "China Energy Statistical Yearbook for the period 2000–2020.

Table 1. Data sources.

Data Type	Data Name	Year	Data Sources URL (accessed on 25 October 2023)
LU data	LU	2000–2020	https://zenodo.org/records/12779975, (accessed on 25 October 2023)
	Dem	2000–2020	https://www.gscloud.cn/, (accessed on 25 October 2023)
socioeconomic development data	Shanghai Statistical Yearbook	2000–2020	https://tjj.sh.gov.cn/tjnj/index.html, (accessed on 25 October 2023)
	Zhejiang Statistical Yearbook	2000–2020	https://tjj.zj.gov.cn/col/col1525563/index.html, (accessed on 25 October 2023)
	Jiangsu Statistical Yearbook	2000–2020	https://www.jiangsu.gov.cn/col/col84736/index.html, (accessed on 25 October 2023)
	Anhui Statistical Yearbook	2000–2020	http://tjj.ah.gov.cn/ssah/qwfbjd/tjnj/index.html, (accessed on 25 October 2023)
	Outline of the 14th FYP for National Economic and Social Development of Jiangsu Province		https://www.jiangsu.gov.cn/art/2021/3/2/art_46143_9684719.html, (accessed on 25 October 2023)
	The 14th FYP for Resource conservation and Circular Economy development in Shanghai		https://www.shanghai.gov.cn/nw12344/20220509/a00971c96ede444eade8000cb9c12766.html, (accessed on 25 October 2023)
	The 14th FYP for the Development of the Circular Economy in Jiangsu Province		https://fzggw.jiangsu.gov.cn/art/2021/9/16/art_83783_10124063.html, (accessed on 25 October 2023)
energy consumption data	China Energy Statistical Yearbook	2000–2020	https://www.stats.gov.cn/, (accessed on 25 October 2023)
	The 14th FYP for Energy Saving and Emissions Reduction in Zhejiang Province		https://fzggw.zj.gov.cn/art/2022/9/6/art_1621019_58934758.html, (accessed on 25 October 2023)
	The 14th FYP for Energy Saving and Emissions Reduction in Anhui Province		https://wjw.ah.gov.cn/group4/M00/03/D1/wKg862LFNjWAesFoAAgU02_m3TU850.pdf, (accessed on 25 October 2023)

2.3. Methods

This study first analyzes the changes in LU in the YRD from 2000 to 2020 utilizing LU data and the LU transfer matrix. Then, by combining energy consumption data with socioeconomic data, the CEs from direct and indirect LU are calculated, applying carbon emission coefficients. Finally, utilizing the extended STIRPAT model along with ridge regression analysis, a carbon emission prediction model in the YRD is constructed by considering the impact of LUCE factors. Using SAs, low-carbon, normal-carbon, and high-carbon situations for LUCE factors from 2021 to 2040 are set based on national policies and previous research results. The prediction model is then used to forecast the time of peak CO_2 emission in diverse scenarios (Figure 2).

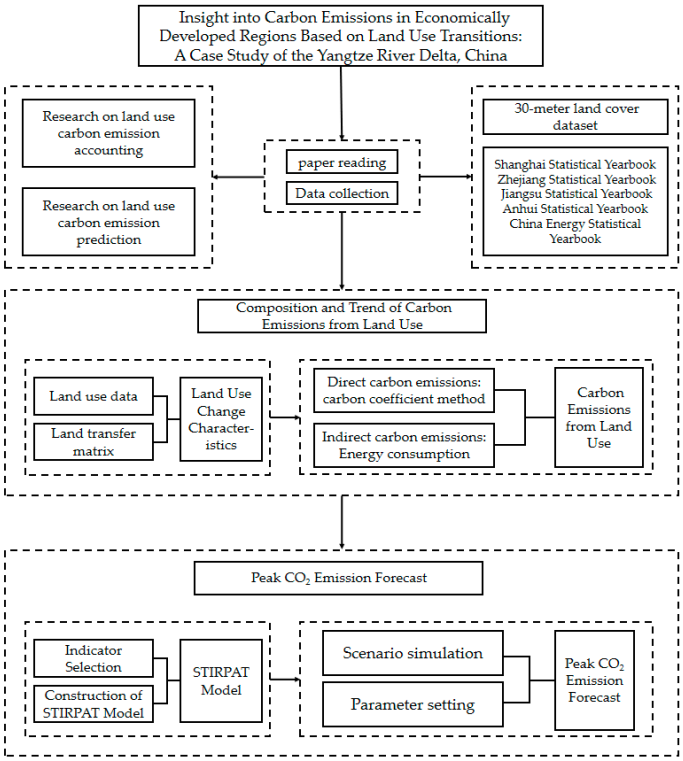

Figure 2. Technical route.

2.3.1. Carbon Emission Calculation for Land Use

LUCEs can be categorized into direct and indirect emissions [37]. The formula for calculation is presented as follows:

$$I = I_d + I_k \tag{1}$$

I represents total CEs, I_d represents direct CEs, and I_k represents indirect CEs. Direct CEs are defined as the CEs produced by specific land types that are directly involved in production, mainly referring to CEs from cropland, forests, grassland, water, and barren lands. The other part is anthropogenic source emissions on the land, that is, indirect CEs [38]. In general, cropland and built-up area are carbon sources, which emit CEs while forest, grassland, water, and barren land are CSs, playing a role in carbon absorption in the carbon cycle [39–41].

With reference to the research outcomes of Fan J, Yuan S, and others [42,43], and combining with the actual circumstances in the YRD, the carbon emission coefficients of cropland, forest, grassland, water and barren land were, respectively, set as 0.422 t/(hm^2·a), −0.644 t/(hm^2·a), −0.021 t/(hm^2·a), −0.253 t/(hm^2·a), −0.005 t/(hm^2·a). The formula for calculation is presented as follows:

$$I_d = \sum(S_i \times \delta_i) \tag{2}$$

S_i denotes the area of the i-th type of LU, and δ_i is the carbon emission coefficient of the i-th LU type.

A large number of production and living activities are carried out on built-up area, so it is impossible to simply and accurately calculate directly.

Instead, It should be calculated by the energy consumption in the use of built-up area [44]; namely, it is characterized through the amount of carbon dioxide generated by energy consumption in production and life. In line with previous studies [45–47], this paper selects nine types of energy sources, including coal, coke, crude oil, gasoline, kerosene, diesel, fuel oil, natural gas, and electricity, to calculate the CEs of built-up area use (Table 2). In China, energy consumption is generally measured in standard coal equivalents. The

energy consumption of the above-mentioned energy sources is therefore first converted into standard coal consumption. CO_2 emissions resulting from energy consumption are then calculated using the following equation:

$$I_k = \sum(E_i \times \theta_i \times f_i) \quad (3)$$

E_i represents the consumption of various energy sources, θ_i represents their coal equivalent coefficients, and f_i represents their carbon emission coefficients.

Table 2. Table of carbon emission coefficients for energy.

Type of Energy	Standard Coal Reference Factor (kgce/kg)	Carbon Emission Factor (tC/tce)
Coal	0.7143	0.7476
Coke	0.9714	0.1128
Crude oil	1.4286	0.5854
Gasoline	1.4714	0.5532
Kerosene	1.4571	0.3416
Diesel	1.4571	0.5913
Fuel oil	1.4286	0.6176
Natural gas	0.13300 kgce/m^3	0.4479
Electricity	0.1229 kgce/kwh	
Source	China Energy Statistical Yearbook	IPCC Guidelines for National Greenhouse Gas Emission Inventories

2.3.2. STIRPAT Model

STIRPAT models are derived from IPAT [48]. The IPAT model was one of the pioneering models to explicitly illustrate how human factors can influence environmental impacts. Ehrlich and Holdren [49] established the theoretical and algebraic foundation for the IPAT, defining total emissions (I) as the product of population (P), per capita GDP (A), and the CEs per unit of GDP (T). The IPAT model succinctly links environmental pressure to these three major factors. However, the IPAT model exhibits constraints in elucidating variations in environmental impacts, as it assumes that the effects of these three factors on environmental impact are linear and proportional [48]. To address this issue, Dietz and Rosa [50] introduced stochastic error terms and variable elasticities in 1994, and proposed the STIRPAT model that enables researchers to more accurately analyze the contributions of different factors to environmental impact and their non-linear relationships, reducing the limitations of the original model. Our study utilizes a STIRPAT model in combination with ridge regression to investigate the elastic correlations among diverse determinants affecting LUCEs in the YRD, and thereby establishes a foundation for forecasting the trends of CEs under various scenarios [51].

(1) Indicator Selection

Based on findings from several previous studies, the driving factors of CO_2 emissions can be summarized into several aspects: economic development level, industrial structure, energy consumption structure, energy efficiency, population size, urbanization rate, and urban-rural structure [15,52–54]. Consequently, this study utilizes the STIRPAT model to analyze the influence of population, GDP per capita, energy intensity, urbanization rate, industrial structure, and energy consumption structure on LUCEs in the YRD (Table 3).

(2) Construction of STIRPAT Model

STIRPAT models are typically based on the following equation [48]:

$$I = aP^b A^c T^d e \quad (4)$$

Table 3. Definition of various variables in the model.

Actual Variable	Symbol	Interpreted Variable	Unit
Population size	P	Residential population in the region	10,000 persons
Affluence	A	GDP per capita	10,000 CNY/person
Energy intensity	T	Energy consumption per unit of regional GDP	Ton of standard coal/CNY 10,000
Energy structure	Es	Coal consumption as a proportion of total energy consumption	%
Industrial structure	Is	The ratio of the value of the secondary industry to the regional GDP	%
Urbanization level	U	Urban population as a percentage of residential population	%

In this context, I, P, A, and T denote environmental impact, population size, affluence level, and technological advancement, respectively; a represents the model coefficient; b, c, and d are the estimated indices; and e signifies the error term. Applying the logarithm to both sides of Equation (4) yields:

$$\ln I = \ln a + b\ln P + c\ln A + d\ln T + \ln e \quad (5)$$

To study the influencing factors of LUCEs in the YRD and based on the actual situation of the region [55], the following model is constructed by extending Equation (5):

$$\ln I = \ln a + b\ln P + c\ln A + d\ln T + f\ln Es + g\ln Is + h\ln U + \ln e \quad (6)$$

where I represents the LUCEs in the YRD (in ten thousand tons); P represents the population size (in ten thousand people); A represents affluence; T represents energy intensity; Es represents the energy structure; Is represents the industrial structure; U denotes the level of urbanization; b, c, d, f, g, and h are the elasticity coefficients that reflect the percentage change in I when P, A, T, Es, Is, and U each increase by 1%; lna represents the constant term; and lne signifies the error term.

(3) Ridge Regression

As there may be multicollinearity among variables, having an adverse effect on the model's accuracy or precision of estimation, the ridge regression method specialized in analyzing collinear data is adopted in this paper to eliminate the collinearity between variables and ensure that the fitting results are more in line with the actual circumstances [56]. This method estimates the standard regression coefficients by adding a set of penalty coefficients k (i.e., the ridge parameter) on the diagonal of the centered explanatory variable matrix. If the ridge parameter k can be reasonably chosen, the mean square error of the result of ridge regression will be significantly reduced. The range of k values varies from 0 to 1, and the smaller the k value, the less information loss and the more accurate the estimation precision. In this study, the distribution range of 0–0.4 was ultimately selected with a search step length of 0.01 to obtain the ridge trace map, when each variable tends to be stable, the corresponding k value is the optimal value.

2.3.3. Scenario Simulation

The SA method refers to assuming multiple possible trends for the forecasted object and conducting forecasts on the development trend in the future [57,58]. This study adopts the SA method to establish low-carbon, normal-carbon, and high-carbon scenarios for the influential factors for LUCEs in the Yangtze River Delta from 2021 to 2040. The first stage is from 2021 to 2025, the second stage is from 2026 to 2030, the third stage is from 2031 to 2035, and the fourth stage is from 2036 to 2040.

For the present study, the normal-carbon scenario is based on the "14th FYP" and the "Long-Range Objectives Through the Year 2035" as well as on the observed change rate in the past decade, to estimate the CEs in each city under the current policy scenario [59,60]. To

model a low-carbon scenario, we set parameters so that they would correspond to relatively minor efforts in terms of taking certain energy conservation and emissions reduction strategies on the basis of current policies from the perspective of sustainable development. Similarly, we set parameters for the high-carbon scenario so that they would correspond to relatively minor failures to meet emission reduction tasks stipulated by current policies. Our choice in setting parameters for the low-carbon scenario was motivated by the assumption that minor improvements would be more feasible and likely to be implemented. For the high-carbon scenario, it was also assumed that minor deviations from policy targets would be more likely to occur, and that it was therefore important to assess the consequences of such deviations in terms of meeting emissions goals. Parameters for the scenarios were set according to the assumptions and metrics described below.

Parameter Setting

This study analyzed the changes in six variables in the STIRPAT model, namely population size (P), affluence (A), energy intensity (T), energy consumption structure (ES), industrial structure (IS), and urbanization level (U), under different scenarios (Table 4).

Table 4. Model variable setting under different scenarios.

Scenario	Year	P (%)	A (%)	T (%)	U (%)	IS (%)	ES (%)
low-carbon	2020–2025	0.12	4.96	−3.37	0.87	−1.5	−3.60
	2025–2030	−0.13	4.03	−3.07	0.78	−1.3	−3.10
	2030–2035	−0.28	2.68	−2.87	0.78	−0.9	−3.10
	2035–2040	−0.38	2.48	−2.67	-	−0.5	−2.47
normal-carbon	2020–2025	0.17	5.42	−2.97	0.87	−1.4	−3.40
	2025–2030	−0.12	4.00	−2.67	0.78	−1.2	−2.90
	2030–2035	−0.27	2.61	−2.47	0.78	−0.9	−2.90
	2035–2040	−0.34	2.17	−2.27	-	−0.5	−2.27
high-carbon	2020–2025	0.13	4.60	−2.57	1.41	−1.2	−3.20
	2025–2030	−0.12	3.86	−2.27	0.76	−0.9	−2.70
	2030–2035	−0.26	2.89	−2.07	0.76	−0.7	−2.70
	2035–2040	−0.35	2.58	−1.87	-	−0.3	−2.07

(1) Population size

From 2016 to 2020, the average natural population growth rate in Shanghai, Zhejiang, Jiangsu, and Anhui was 0.19%, 1.34%, 0.35%, and 0.32%, respectively. Meanwhile, population economists forecast that China will begin to experience negative population growth by 2030. Combined with Wang Can's [61] population forecast for China's provinces for 2010–2100 under five socioeconomic development scenarios, this study used SSP1 as the low-carbon scenario, SSP2 as the normal-carbon scenario, and SSP5 as the high-carbon scenario. The average annual growth rate of population size is set as 0.17%, −0.12%, −0.27%, and −0.34% for 2020–2025, 2025–2030, 2030–2035, and 2035–2040, respectively, in the normal-carbon scenario. For the low-carbon scenario, the rates are 0.12%, −0.13%, −0.28%, and −0.38%, respectively, while for the high-carbon scenario, they are 0.13%, −0.12%, −0.26%, and −0.35%.

(2) Affluence

According to the "Outline of the 14th Five-Year Plan (FYP) for National Economic and Social Development of Jiangsu Province" (2020–2025), the GDP per capita is expected to exceed CNY 150,000 by 2025. Anhui Province has set a goal of CNY 90,000 for GDP per capita by 2025 with an annual growth rate of 5.6%, while Zhejiang Province aims to exceed CNY 130,000. Combining Jiang Tong and Zhao Jing's [62] economic forecast results for each province under the shared socioeconomic development path, as well as Wang Can's population forecast, the average annual growth rates of GDP per capita are set as 5.42%, 4.00%, 2.61%, and 2.17% for 2020–2025, 2025–2030, 2030–2035, and 2035–2040, respectively,

in the normal-carbon scenario. For the low-carbon scenario, the rates are 4.96%, 4.03%, 2.68%, and 2.48%, respectively, and for the high-carbon scenario, they are 4.60%, 3.86%, 2.89%, and 2.58%, respectively.

(3) Energy intensity

According to "The 14th FYP for Resource conservation and Circular Economy development in Shanghai", the energy consumption per unit of GDP is expected to decrease by 14% from 2020 to 2025. The "14th FYP for the Development of the Circular Economy in Jiangsu Province" stipulates that the energy consumption per unit of land GDP will decrease by 15% in 2025 compared to 2020. The "14th FYP for Energy Saving and Emissions Reduction in Zhejiang Province" requires that the energy consumption per unit of GDP will decrease by 14.5% in 2025 compared to 2020, and the "14th FYP for Energy Saving and Emissions Reduction in Anhui Province" aims to reduce energy consumption per unit of land GDP by 14% by 2025, striving to decrease by 14.5%. Therefore, in the normal-carbon scenario, the average annual change rate of energy intensity in the YRD from 2020 to 2025 is set to decrease by 14%, with an annual change rate of −2.97%. As energy structure adjustment and energy utilization efficiency improve, the decrease rate of energy intensity will gradually slow down. Following the mainstream setting method of declining annual change rates across the period [63–65], the annual change rate will increase by 0.3%, 0.5%, and 0.7% from 2026 to 2030, 2031 to 2035, and 2036 to 2040, respectively. The energy intensity change rates for the high-carbon (+0.4%) and low-carbon (−0.4%) scenarios are also established based on the normal-carbon scenario.

(4) Urbanization level

According to the "14th FYP for Economic and Social Development" in Shanghai, Zhejiang, Jiangsu, and Anhui provinces, the urbanization rate target for 2025 is 90%, 75%, 75%, and 65%, respectively. The urbanization rates in each province are projected to attain 90%, 80%, 80%, and 70% by 2035, respectively, in accordance with the long-term development targets. Therefore, the urbanization rate is set to 74% in the low-carbon and normal-carbon scenarios for 2025, with an annual growth rate of 0.87%, and the rate is set to 80% in 2035, with an annual growth rate of 0.78%. In the high-carbon scenario, the urbanization rate is set to 76% in 2025 and 82% in 2035, with annual growth rates of 1.41% and 0.76%, respectively, while the urbanization rate remains stable from 2035 to 2040.

(5) Industrial structure

From 2015 to 2020, the changes in the proportion of the second industry to the GDP in Shanghai, Jiangsu, Zhejiang, Anhui, and the entire YRD are −3.38%, −1.51%, −2.96%, −2.55%, and −2.27%, respectively. Combined with the long-term development goals for 2035 and the ideal proportion of the secondary industry to GDP of 35% in developed countries, the average annual change rate of the proportion of the secondary industry to GDP is set as −1.4%, −1.2%, −0.9%, and −0.5% for 2020–2025, 2025–2030, 2030–2035, and 2035–2040, respectively, in the normal-carbon scenario. For the low-carbon scenario, the corresponding rates are −1.5%, −1.3%, −0.9%, and −0.5%, while for the high-carbon scenario, they are −1.2%, −0.9%, −0.7%, and −0.3%, respectively.

(6) Energy consumption structure

According to the "China Energy Revolution Progress Report (2020)", the proportion of coal in primary energy consumption was approximately 57.7% in 2019 [66], with an average annual decrease rate of 2.44% from 2015. It is expected that the proportion of coal will drop to below 50% by the end of the "14th FYP" (2025), with an average annual decrease rate of 2.36%. Global and China Energy Outlook (2050) estimates that the proportion of coal and carbon in China will be around 30.7% in 2050 [67], with an average annual decrease rate of 1.93% from 2025. The data indicates that between 2015 and 2020, the annual rate of decline in coal consumption in the YRD was 3.52%. Therefore, the energy consumption structure change rate in the YRD from 2020 to 2025 in the normal-carbon scenario is set to be −3.40%, and that from 2025 to 2035 is −2.90%. The change rate from 2035 to 2040 is −2.27%. The

high-carbon (+0.2%) and low-carbon (−0.2%) scenarios for energy consumption structure are also established based on the normal-carbon scenario.

3. Results

3.1. Land Use Structure Characteristics

LU classification maps were generated using ArcGIS 10.6 (Figure 3), and the area for each LU type was computed to create Table 5. The area change rate in Table 5 is the ratio of the changed area of different LUs in the past 20 years to the area in 2000.

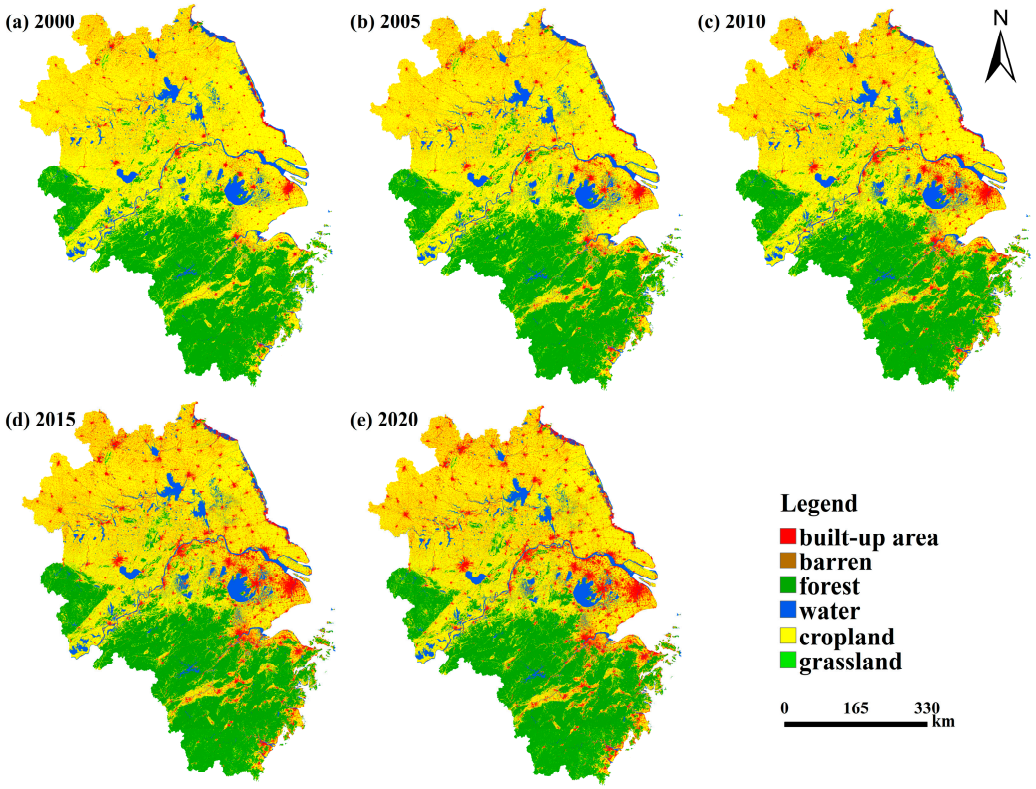

Figure 3. Land use classification map for the YRD for the period 2000–2020.

Table 5. Land use structure of the YRD.

Unit: Hectares	Cropland	Forest	Grassland	Water	Barren Land	Built-Up Area	Total Area
2000	19,825,127.64 56.11%	10,801,425.69 30.57%	18,417.33 0.05%	2,257,165.89 6.39%	1980.00 0.01%	2,425,394.70 6.87%	35,329,511.70
2005	19,163,908.35 54.24%	10,902,312.99 30.86%	15,719.85 0.04%	2,405,254.59 6.81%	956.25 0.00%	2,841,359.58 8.04%	35,329,511.70
2010	18,593,248.14 52.63%	10,923,399.90 30.92%	16,518.60 0.05%	2,414,010.51 6.83%	676.71 0.00%	3,381,657.84 9.57%	35,329,511.70
2015	18,304,264.80 51.81%	10,618,661.97 30.06%	10,739.43 0.03%	2,381,475.78 6.74%	474.48 0.00%	4,013,895.24 11.36%	35,329,511.70
2020	18,247,108.14 51.65%	10,506,782.43 29.74%	5084.55 0.01%	2,209,391.55 6.25%	424.71 0.00%	4,360,720.32 12.34%	35,329,511.70
20-year area change	−1,578,019.5	−294,643.26	−13,332.78	−47,774.34	−1555.29	1,935,325.62	
Rate of area change	−7.96%	−2.73%	−72.39%	−2.12%	−78.55%	79.79%	

From Table 5, it can be discerned that the principal LU types in the YRD are cropland, forest, and built-up area. Cropland is the largest, with an area of 18,247,108.14 hectares in 2020, representing approximately fifty percent of the overall area of the study region. However, the area of cropland has been declining annually and is primarily located in the northern section of the YRD, specifically in Jiangsu and Anhui provinces. The second is

forest; its area was 10,506,782.43 hectares in 2020, constituting approximately 30% of the overall area. Between 2000 and 2010, the forested area experienced a gradual increase, but it began to decrease gradually after 2010, chiefly distributed in the southern portion of the YRD urban agglomeration. (Zhejiang Province). The built-up area is centered around Shanghai and radiates continuously from the water system along the river, with its area increasing from 6.87% of the total area in 2000 to 12.34%, reaching 4,360,720.32 hectares in 2020. The rate of change in the built-up area is as high as 79.79%. Within the six categories of LU, only the area of built-up area increased, and all other types of land decreased, with the largest decrease being in barren land and grassland, with area change rates of −78.55% and −72.39%, respectively.

3.2. Land Use Change Characteristics

Based on ArcGIS 10.6, a quantitative analysis was conducted on the characteristics of LU changes in the study area, and the LU transition matrixes from 2000 to 2005, from 2005 to 2010, from 2010 to 2015, from 2015 to 2020, and from 2000 to 2020 were obtained (Table 6 and Figure 4). For the aspect of LU transition direction, a total of 3,970,175.13 hectares of land were mutually converted between 2000 and 2020. In the LU outbound transition process, cropland had the largest converted area, followed by forest, water, built-up area, and grassland, while the converted area of barren land was the smallest. In the LU inbound transition process, built-up area had the largest converted area, followed by cropland, water, forest, and grassland. From the perspective of the net converted area, only the extent of built-up area significantly increased, whilst all other LU categories witnessed a decrease. (Table 6).

From 2000 to 2020, built-up area expanded considerably, by a total of 1,935,325.62 hectares (Table 5). Specifically, the area of added built-up area increased every five years from 2000 to 2015, reaching a peak in 2010–2015, before declining slightly in 2015–2020 with a 44.53% decrease compared to the previous period. As shown in Table 5, the majority (around 90%) of the converted built-up area came from cropland due to accelerated urbanization and industrialization with the start of the 1990s. This resulted in a large number of croplands being converted to built-up areas as agricultural land was transferred. Additionally, waters accounted for 6–10% of the converted land while 2% was converted from forest.

Between 2000 and 2020, a total of 2,497,602.60 hectares of cropland flowed into built-up area, with the percentage flowing to built-up area increasing from 44.91% in 2000–2005 to 55.61% in 2005–2010, and further to 68.25% in 2010–2015, before dropping to 55.75% in 2015–2020. During the same period, some cropland was also converted into forest and waters. The proportion of cropland converted to forest decreased gradually from 28.14% in 2000–2005 to 13.22% in 2010–2015 before sharply increasing to 29.26% in 2015–2020 due to the implementation of the "Regulations on Returning Cropland to Forests" [68] in 2002. However, in 2007, the State Council issued a notice to suspend this policy in order to avoid encroaching on the red line of 1.8 billion mu of cropland. It was not until 2014 that the policy was restarted under the "Overall Plan for Returning Cropland to Forests and Grasslands". Consequently, the primary factor behind the decrease in cropland is the transformation of agricultural land into built-up areas, along with the national policy aimed at converting cropland back to forested areas, which also plays a role in this decline.

3.3. Composition and Trend of LUCEs

Between 2000 and 2020, the LUCEs in the YRD manifested a continuous upward trajectory, escalating from 2.70×10^8 t in 2000 to 9.10×10^8 t in 2020, with an increase of about 6.4×10^8 t, an increase rate of 243.77%. However, the increase rate for every five years showed a significant downward trend, being 75.16%, 46.78%, 18.08%, and 13.24%, respectively, indicating that the CEs problem has been paid attention to for a long time. When considering the carbon sources, human activities in the built-up area were the dominant carbon source, accounting for 96.90% of the total CEs in 2000. The emissions showed a constant growth trend over the past 20 years, breaking through 98% of total CEs

in 2005, and accounting for 99.15% of total CEs in 2020. It can be seen that almost all CEs are derived from built-up areas. Looking at the CSs, forests were the primary contributors, representing over 90% of the overall carbon sink. Due to its strong carbon sink capacity, and the forest maintaining at around 30% of the regional total area, its carbon absorption effect is very significant. (Table 7).

Table 6. 2000–2020 land use transfer matrix.

Unit: Hectares					**2005**			
	LU Type	**Cropland**	**Forest**	**Grassland**	**Water**	**Barren Land**	**Built-Up Area**	**Transfer-Out Area**
2000	Cropland	18,887,908.14	263,699.73	2808.81	249,769.62	4.14	420,937.2	937,219.5
	Forest	155,996.73	10,635,583.59	70.65	152.46	0	9622.26	165,842.1
	Grassland	3904.83	669.51	12,627.99	154.08	35.82	1025.1	5789.34
	Water	114,509.61	2359.35	75.87	2,112,064.83	94.77	28,061.82	145,101.42
	Barren land	175.77	0	136.53	357.12	820.71	489.87	1159.29
	Built-up area	1413.27	0.81	0	42,756.48	0.81	2,381,223.33	44,171.37
	Transfer-in area	276,000.21	266,729.4	3091.86	293,189.76	135.54	460,136.25	1,299,283.02
					2010			
2005	Cropland	18,249,230.34	222,782.67	5012.64	178,225.29	21.87	508,635.54	914,678.01
	Forest	191,744.28	10,698,219.9	168.57	182.79	0	11,997.45	204,093.09
	Grassland	2433.6	596.61	11,168.46	81.36	177.66	1262.16	4551.39
	Water	148,982.49	1795.14	139.77	2,204,361.27	138.78	49,837.14	200,893.32
	Barren land	66.96	0	28.8	132.84	338.22	389.43	618.03
	Built-up area	789.84	4.05	0.36	31,026.78	0.18	2,809,538.37	31,821.21
	Transfer-in area	344,017.17	225,178.47	5350.14	209,649.06	338.49	572,121.72	1,356,655.05
					2015			
2010	Cropland	17,733,922.65	166,901.67	515.88	84,959.73	1.89	317,960.1	570,339.27
	Forest	273,837.33	10,338,709.95	104.85	122.94	0	5886.63	279,951.75
	Grassland	4490.01	971.91	4446.18	27.27	69.21	734.94	6293.34
	Water	234,345.96	198.36	6.48	2,109,282.57	137.16	37,504.62	272,192.58
	Barren land	62.55	0.09	10.98	23.22	215.91	161.73	258.57
	Built-up area	446.85	0.81	0.18	14,975.64	0.54	3,998,474.82	15,424.02
	Transfer-in area	513,182.7	168,072.84	638.37	100,108.8	208.8	362,248.02	1,144,459.53
					2020			
2015	Cropland	17,733,922.65	166,901.67	515.88	84,959.73	1.89	317,960.1	570,339.27
	Forest	273,837.33	10,338,709.95	104.85	122.94	0	5886.63	279,951.75
	Grassland	4490.01	971.91	4446.18	27.27	69.21	734.94	6293.34
	Water	234,345.96	198.36	6.48	2,109,282.57	137.16	37,504.62	272,192.58
	Barren land	62.55	0.09	10.98	23.22	215.91	161.73	258.57
	Built-up area	446.85	0.81	0.18	14,975.64	0.54	3,998,474.82	15,424.02
	Transfer-in area	513,182.7	168,072.84	638.37	100,108.8	208.8	362,248.02	1,144,459.53
					2020			
2000	Cropland	17,327,525.04	347,408.64	535.50	340,071.48	122.85	1,809,464.13	2,497,602.60
	Forest	586,735.38	10,152,806.04	925.38	3231.81	20.52	57,706.56	648,619.65
	Grassland	9195.21	2854.35	3593.97	337.59	48.51	2387.70	14,823.36
	Water	302,284.89	3795.12	18.90	1,810,406.52	140,660.82	280,618.20	727,377.93
	Barren land	365.67	0.27	8.28	742.77	8207.10	4898.70	6015.69
	Built-up area	20,999.16	69.84	2.52	54,601.20	63.18	799.83	75,735.90
	Transfer-in area	919,580.31	354,128.22	1490.58	398,984.85	140,915.88	2,155,075.29	3,970,175.13

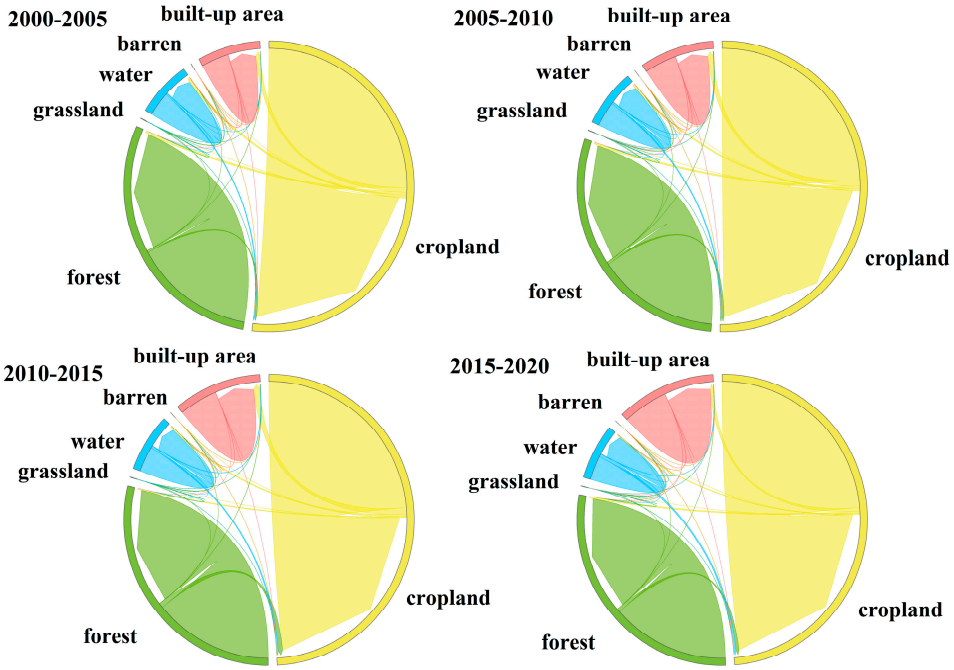

Figure 4. Chord diagram of land use for the period 2000–2020.

Table 7. LUCEs/carbon absorption.

Year	LUCEs/Carbon Sequestration (t)								Net CEs
	Carbon Source	Built-Up Area	Cropland	Carbon Sink	Forest	Grassland	Water	Barren Land	
2000	270,122,768.2	261,756,564.3 96.903%	8,366,203.9 3.097%	−7,527,577.8	−6,956,118.1 92.41%	−386.8 0.005%	−571,063.0 7.586%	−9.9 0.000%	262,595,190.4
2005	467,593,483.8	459,506,314.5 98.270%	8,087,169.3 1.730%	−7,629,953.9	−7,021,089.6 92.02%	−330.1 0.004%	−608,529.4 7.976%	−4.8 0.000%	459,963,529.9
2010	682,774,771.4	674,928,420.7 98.851%	7,846,350.7 1.149%	−7,645,764.5	−7,034,669.5 92.01%	−346.9 0.005%	−610,744.7 7.988%	3.4 0.000%	675,129,006.9
2015	804,606,581.1	796,882,181.4 99.040%	7,724,399.7 0.960%	−7,441,159.6	−6,838,418.3 91.90%	−225.5 0.003%	−602,513.4 8.097%	−2.4 0.000%	797,165,421.5
2020	910,036,908.1	902,336,628.5 99.154%	7,700,279.6 0.846%	−7,325,452.8	−6,766,367.9 92.37%	−106.8 0.001%	−558,976.1 7.631%	−2.1 0.000%	902,711,455.3

Focusing solely on the changes in carbon sources, emissions from built-up areas rose sharply from 2.62 × 10^8 t in 2000 to 9.02 × 10^8 t by 2020, representing an increase of approximately 6.41 × 10^8 t and a growth rate of 244.72%. The increase rates in the past two decades were 75.55%, 46.88%, 18.07%, and 13.23%, respectively. Meanwhile, the carbon emission coefficients for built-up area were 10.79 kg·m^{-2}·a^{-1}, 16.17 kg·m^{-2}·a^{-1}, 19.96 kg·m^{-2}·a^{-1}, 19.85 kg·m^{-2}·a^{-1}, and 20.69 kg·m^{-2}·a^{-1} in 2000, 2005, 2010, 2015, and 2020, respectively, with an always increasing trend. However, the increasing trend in 2010–2020 was significantly reduced. It is evident that the rate of increase in CEs from the built-up area is essentially in accordance with the trend of net LUCEs. In addition, according to Table 2, built-up area increased by about 79.79% between 2000 and 2020, while CEs from this area rose by around 244.72%, which is much larger than the change in area. This implies that the enlargement of the area is not the predominant cause for the rise in CEs from built-up areas. CEs from agricultural land exhibited a gradual decline, decreasing from 8.37 × 10^6 t in 2000 to 7.70 × 10^6 t in 2020, with a decrease of about 6.66 × 10^5 t, a decrease rate of 8.65%. This is primarily attributed to the reduction in cropland area resulting from urbanization, leading to a reduction in CEs from cropland.

Regarding the CSs, the total quantity of carbon absorption manifested a slow upward trend and then a downward trend, rising by only 11.81 × 10^4 tons from 2000 to 2010. After

2010, the total amount of carbon absorption began to decline and decreased by 32.03 × 10^4 t compared with the amount in 2010 by 2020.

3.4. Peak CO_2 Emission Forecast

3.4.1. Impact Mechanism of Carbon Emissions

To eliminate the multicollinearity and accurately estimate the regression coefficients, testing for multicollinearity among the explanatory variables is important. In this study, SPSS 25 was used to diagnose the collinearity among the variables. Should the results indicate that the VIF of each variable is greater than 10, it indicates that there are significant correlations among them (Table 8). Therefore, we employed ridge regression to analyze the variables and improve the accuracy of the fit.

Table 8. LUCEs/carbon absorption.

Coefficient [a]							
Model	**Unstandardized Coefficient**		**Standardized Coefficient**	**t**	**Significance**	**Collinearity Statistics**	
	B	**Standard Error**	**Beta**			**Tolerance**	**VIF**
(Constant)	−7.257	5.030		−1.443	0.171		
lnP	1.853	0.506	0.263	3.662	0.003	0.003	373.481
lnA	0.692	0.081	1.102	8.530	0.000	0.001	1207.704
lnT	0.615	0.090	0.621	6.827	0.000	0.002	599.258
lnEs	0.355	0.071	0.076	5.015	0.000	0.061	16.499
lnIs	0.456	0.142	0.100	3.269	0.00 6	0.015	67.377
lnU	0.921	0.201	0.367	4.578	0.000	0.002	465.864

[a] Dependent variable: lnI.

Based on the ridge trace graph and ridge regression estimates, when the value of k was around 0.02, the ridge trace graph became stable (Figure 5), with R^2 = 0.997, F value = 1312.596, and Sig F = 0.000 (Table 9). It can be seen that when k is equal to 0.02, ridge regression demonstrates a relatively strong fitting effect, and the model performs well. Therefore, the STIRPAT model equation can be established that:

$$\ln I = -7.055 + 1.932\ln P + 0.241\ln A - 0.141\ln T + 0.043\ln Es + 1.440\ln Is + 1.045\ln U \quad (7)$$

According to the regression equation, population size, GDP per capita, energy consumption structure, industrial structure, and urbanization rate all significantly promote LUCEs in the YRD. Meanwhile, the elasticity coefficients of each variable are different. Population and industrial structure exert a predominant role in promoting CEs, with correlation coefficients of 1.932 and 1.440, respectively, and only energy intensity exhibits a negative relationship, indicated by a correlation coefficient of −0.141.

The real values of the six variables were substituted into the equation, and the fitted values during the study period were compared with the actual values. The findings suggest that the errors were within reasonable ranges, demonstrating a high estimated accuracy for the equation (Table 10).

The growth of the population size constitutes a decisive element giving rise to the rise in LUCEs in the YRD. This is due to the coordinated development of the YRD, which makes the region have a strong comprehensive competitiveness, and excellent economic and social development conditions. On the one hand, the high level of urban development attracts a large number of outstanding talents and external population inflows, thereby increasing energy consumption in industries such as electricity, transportation, and real estate, which gives rise to an escalation in CEs. On the other hand, the abundant labor force stimulates the region's economic level and the increases in residents' living standards, and as such the consumption of living resources and the utilization of production materials have significantly increased, thereby driving an increase in the social carbon footprint. The industrial structure constitutes the second principal factor impacting the augmentation of

LUCEs in the YRD, so optimization of industrial-structure adjustment remains as having significant potential. At the same time, the CEs produced by land designated for the secondary industry exceed those from land allocated to the tertiary industry, so shifting from secondary to tertiary industry can be a useful industrial development strategy to achieve the objectives of energy efficiency and emission reduction. Reducing energy intensity is the primary method for decreasing CEs. This is due to the enhancement of technological advancements, and can augment the efficiency of energy consumption, thus decreasing energy usage per unit of production and reducing the production of greenhouse gasses from both the perspective of reducing energy use and increasing energy utilization efficiency.

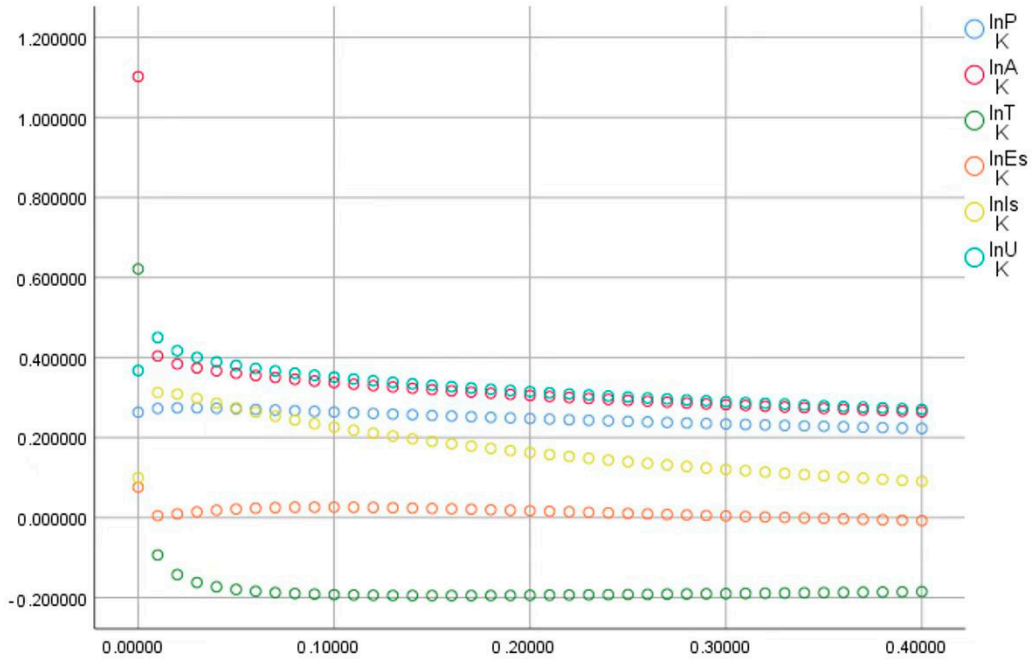

Figure 5. Ridge trace map.

Table 9. Ridge regression estimation results.

K = 0.02	Unstandardized Coefficient		Standardized Coefficient	t	P	R^2	Adjusted R^2	F
	B	Standard Error	Beta					
lne	−7.055	1.457	-	−4.841	0.000 **	0.998	0.997	1312.596 (0.000 ***)
lnP	1.932	0.147	0.274	13.171	0.000 **			
lnA	0.241	0.008	0.384	28.429	0.000 **			
lnT	−0.141	0.021	−0.143	−6.700	0.000 **			
lnEs	0.043	0.123	0.009	0.350	0.731			
lnIs	1.440	0.107	0.309	13.460	0.000 **			
lnU	1.045	0.053	0.417	19.599	0.000 **			

Sig F = 0.000 Dependent variable: lnI. ***, ** represent significance levels of 1%, 5%, respectively.

3.4.2. Estimated Results

In the contexts of low-carbon, normal-carbon, and high-carbon scenarios, peak carbon dioxide emission years for land use emission are 2025, 2030, and 2035, respectively, with peak values of 9.10×10^8 t, 9.25×10^8 t, and 9.73×10^8 t (Figure 6). By comparing the trends of LUCEs across the three scenarios, it was observed that the overall trends of CEs are similar, with varying degrees of growth before peaking, influenced by multiple driving factors. From 2021 to 2025, LUCEs rose considerably across all scenarios, with the highest increase observed in the high-carbon scenario, while the low-carbon scenario exhibited the smallest increase and peaked in 2025. The normal-carbon scenario's growth rate was

between the high-carbon and low-carbon scenarios. From 2025 to 2030, LUCEs continued to surge in the high-carbon scenario, but growth rates reduced compared to 2021–2025. The normal-carbon scenario also witnessed a surge, but the growth rate significantly slowed down until reaching its peak in 2030. In the period 2030–2035, only the high-carbon scenario experienced further carbon emission growth, reaching its peak in 2035.

Table 10. Comparison of actual and model-fitted values for LUCEs.

Year	Estimated Value (10,000 t)	Actual Value (10,000 t)	Error (10,000 t)	Error Rate
2000	26,708.27682	26,259.51904	448.757783	1.71%
2001	28,049.94751	27,552.99544	496.9520668	1.80%
2002	30,388.69287	30,325.19704	63.49583408	0.21%
2003	35,207.96022	34,725.96306	481.9971626	1.39%
2004	39,987.67096	39,698.80429	288.8666693	0.73%
2005	44,608.30471	45,996.35299	−1388.048287	3.02%
2006	49,190.87637	50,234.03399	−1043.157616	2.08%
2007	53,857.97537	55,305.93724	−1447.961871	2.62%
2008	57,855.52602	58,118.93629	−263.4102744	0.45%
2009	58,969.61993	60,949.58582	−1979.96589	3.25%
2010	67,178.07468	67,512.90069	−334.8260093	0.50%
2011	73,138.92969	73,735.02692	−596.097226	0.81%
2012	75,047.18413	75,403.41951	−356.2353785	0.47%
2013	77,245.17226	78,938.74086	−1693.568593	2.15%
2014	80,152.61260	78,487.29450	1665.3181040	2.12%
2015	80,109.09632	79,716.54215	392.5541658	0.49%
2016	80,425.21205	82,763.35098	−2338.13893	2.83%
2017	84,981.86767	85,339.10985	−357.2421739	0.42%
2018	88,627.34692	87,183.61181	1443.735117	1.66%
2019	88,835.10881	88,758.82526	76.28355544	0.09%
2020	88,862.12205	90,271.14553	−1409.023474	1.56%

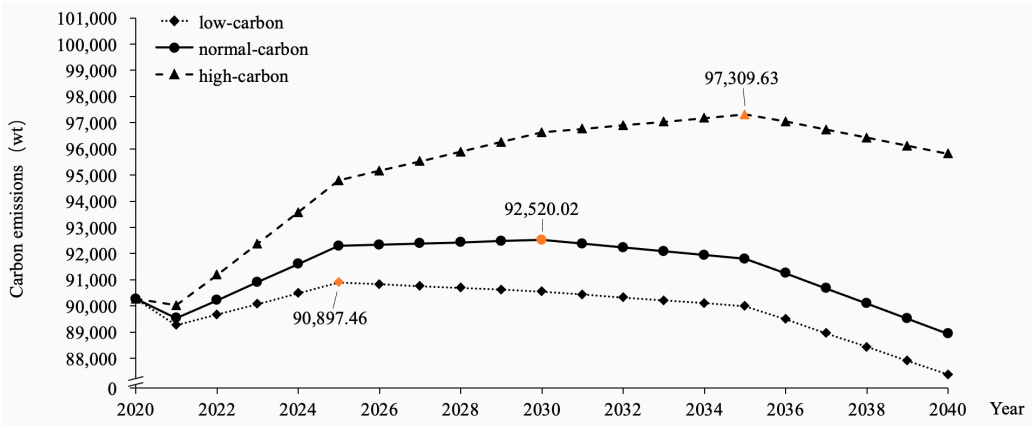

Figure 6. Change trend in LUCEs during 2020–2040 under L-N-H scenarios.

4. Discussion

(1) With the increasingly severe issue of CEs, it is crucial to establish effective carbon emission prediction models (CEPM) to forecast emission trends in carbon dioxide. In existing research on CE forecasts, different models use different conditions and exhibit different performances. The Gray Forecast Model can be easily combined with other models, has a simple calculation method, and high accuracy, but is suitable for forecasting only in the short and medium term. The environmental Kuznets curve examines the connection between economic growth and the quality of the environment, but the factors affecting LUCEs are not exclusively linked to economic aspects. Although the ARIMA and neural network models have the advantage of more accurate prediction results, they are relatively weak in explaining the specific effects of emission reduction measures.

The aim of our study was to assess the role of current policies in China in CE reduction, test the effectiveness of policies, and use the STIRPAT model to quantitatively calculate the impact of human behaviors, such as those regarding population, economy, and technology, on the environment. The variables involved in the STIRPAT model are macro-variables, making it convenient to set scenario parameters and possessing high flexibility and scalability, making it more suitable for evaluating the effects of measures for reducing emissions. Simultaneously, this model is capable of clearly revealing the most sensitive factors among the factors that affect CEs and exerting a more significant role in policy guidance. However, the scenario and parameter setting process is relatively complex and the parameters need to be reasonably set according to a large number of recent and long-term policies.

(2) Due to the increasing attention and requirements for energy conservation and emission reductions in current development policies, it is feasible to achieve the goal of peaking carbon dioxide emissions in 2030, with the peak value of 9.10×10^8 t, under the normal-carbon scenario. However, there are both mandatory and expected indicators in the existing planning policies, which require strict adherence to planning requirements by local governments in order to achieve China's goal of peaking carbon dioxide emissions by 2030. In the low-carbon scenario, adjustments are made to energy and industrial structure, and energy efficiency is improved through technological advancement. With sustained economic development, population transformation, and upgrading, it would be possible to achieve carbon peaking ahead of schedule in 2025, with the peak value of 9.25×10^8 t, which is a 1.75% reduction compared to the normal-carbon scenario. However, in the high-carbon scenario, if current policies were not to be effectively implemented, energy efficiency were not improved, and if economic development were to rely on fossil fuels to a greater extent than anticipated in policy targets, then the CEs from built-up areas would not be effectively controlled, resulting in continuous increase in CEs. Under the high-carbon scenario, carbon peaking would not be achieved until 2035, with the peak value of 9.73×10^8 t, which is a 5.18% increase compared to the normal-carbon scenario. Overall, both the normal-carbon and low-carbon scenarios are capable of achieving carbon peaking in the YRD by 2030. However, as this paper only considers LUCEs, achieving carbon peaking before 2030 is a better choice. The low-carbon scenario balances both social development needs and CE reduction, which is a feasible low-carbon pathway for the YRD. In addition, in the upcoming urbanization process in the region, there will inevitably be a phenomenon of urban expansion encroaching on urban and rural ecological space. Therefore, in the process of suppressing carbon source growth, the weakening of CSs should also be avoided, and the maintenance of carbon sink capacity should be addressed.

(3) Compared with previous studies on LUCE estimation [12,13], despite differences in study regions, scales, and estimation methods used, they all conclude that CEs from built-up area are the main source of carbon and that forest land plays a dominant role in carbon absorption. This paper further validates this conclusion through the utilization of the carbon emission coefficient method for the calculation of LUCEs in the YRD. Additionally, relevant studies have demonstrated that the factors influencing LUCEs in the area comprise population size, urbanization rate, GDP per capita, industrial structure, and energy consumption [24,69], with different intensities of influence attributed to disparate levels of regional economic development, urbanization stages, and development models. As for forecasting of CO_2 emission peaks, studies have mainly focused on the normal-carbon scenario within the region, with peak years ranging from 2025 to 2030 [24,51], and cities with higher economic development levels tend to reach carbon peaking earlier. For the YRD, previous studies have estimated that its CEs will peak in 2020, 2025, and 2040 under low-carbon, normal-carbon, and high-carbon scenarios, respectively [70]. However, as this study did not solely take into account the CEs produced by energy use in built-up areas, but also took into account the process of carbon cycling in other LU types, and as such there may be differences in the estimated results.

(4) This study investigates CEs' effect in terms of LU, clarifies the direction and intensity of the factors influencing LUCEs in the YRD, and simplifies the complex mechanism of

LUCE changes. By forecasting the trends in LUCEs at a macro level based on the changing rates of various indicators according to the three scenarios set by local policies, this paper provides an important intervention approach for regulating CEs from macro-level socioeconomic activities. It could be a valuable reference for advancing carbon peaking and carbon neutralization goals, improving LU management policies, and optimizing technological conditions in order to achieve carbon reduction.

(5) However, the CE calculation presented in this paper merely considers diverse LUCE coefficients and selected energy consumption data, disregarding the differences in carbon emission coefficients caused by regional and temporal circumstances, as well as all anthropogenic CEs on land carriers at a more comprehensive level, leading to a certain level of discrepancy from actual CEs. In addition, this paper only selects macro-level socioeconomic data as factors affecting LUCEs, weakening the impact of changes in LU structures on CEs and failing to forecast future LUCEs by estimating future trends in land structure changes. Nevertheless, this paper offers an occasion for subsequent exploration, from the perspectives of human activities and natural processes, of how LU changes influence the transformation of land management practices, alterations in the patterns of artificial energy consumption, and the resultant variations in LUCEs, and for in-depth examination of the underlying mechanism by which LU affects CEs. It also offers novel research perspectives and directions for attaining a decrease in CEs going forward from the perspectives of optimizing LU structure and territorial spatial layout.

5. Conclusions

(1) LU in the YRD is predominantly characterized by cropland, which accounts for over 50% of the total land area. From 2000 to 2020, the overall trend of LU change involves a decrease in cropland, forest, grassland and water, with the largest decrease being in cropland. Meanwhile, built-up area has increased, with a growth rate of 79.79% over the 20 years. The main reason is the rapid economic development and urbanization process in the YRD, which has led to accelerated expansion of urban areas and transfer of land from agriculture to construction [71]. Built-up areas constitute the primary contributor to CEs, contributing more than 96% to net CEs and demonstrating the highest correlation with total CEs. On the contrary, the forest serves as the primary carbon sink, contributing over 91% to carbon sequestration.

(2) Over the course of the past two decades, the LUCEs in the YRD have manifested a continuous upward tendency, yet the rate of escalation has gradually decelerated. Population size, per capita GDP, energy consumption structure, industrial structure, and urbanization rate all exert a positive promoting impact on LUCEs within the region, with population size having the greatest effect, followed by industrial structure, urbanization rate, GDP per capita, and energy consumption structure. Only energy intensity demonstrates a negative correlation with the LUCEs.

(3) Under the low-carbon, normal-carbon, and high-carbon scenarios, the YRD will achieve carbon peaking in 2025, 2030, and 2035, respectively, with peak values of 9.10×10^8 t, 9.25×10^8 t, and 9.73×10^8 t. It should also be noted that peaking CO_2 emissions in China by 2030 may still be insufficient to remain within safe planetary boundaries.

Author Contributions: Conceptualization, Y.L. and Y.Z.; methodology, Y.L.; software, Y.L.; validation, Y.Z. and X.L.; formal analysis, Y.L. and Y.Z.; investigation, Y.L.; resources, Y.Z. and X.L.; data curation, Y.L., Y.Z. and X.L.; writing—original draft preparation, Y.L.; writing—review and editing, Y.L.; visualization, Y.L.; supervision, Y.Z.; project administration, Y.Z.; funding acquisition, Y.L., Y.Z. and X.L. All authors have read and agreed to the published version of the manuscript.

Funding: This research was funded by the Postgraduate Innovation Research Scheme Project of the National Natural Science Foundation of China, grant number 42171328.

Data Availability Statement: Dataset available on request from the authors.

Acknowledgments: Thank you to everyone who contributed to this study. We appreciate the constructive comments from the reviewers to improve the quality of this manuscript.

Conflicts of Interest: The authors declare no conflicts of interest.

References

1. Hansen, J.; Sato, M.; Russell, G.; Kharecha, P. Climate sensitivity, sea level and atmospheric carbon dioxide. *Philos. Trans. A Math. Phys. Eng. Sci.* **2013**, *371*, 20120294. [CrossRef] [PubMed]
2. Jones, M.W.; Kelley, D.I.; Burton, C.A.; Di Giuseppe, F.; Barbosa, M.L.F.; Brambleby, E.; Hartley, A.J.; Lombardi, A.; Mataveli, G.; McNorton, J.R.; et al. State of wildfires 2023–2024. *Earth Syst. Sci. Data* **2024**, *16*, 3601–3685. [CrossRef]
3. McKay, D.I.A.; Staal, A.; Abrams, J.F.; Winkelmann, R.; Sakschewski, B.; Loriani, S.; Fetzer, I.; Cornell, S.E.; Rockström, J.; Lenton, T.M. Exceeding 1.5 C global warming could trigger multiple climate tipping points. *Science* **2022**, *377*, eabn7950. [CrossRef] [PubMed]
4. Harmsen, M.; Tabak, C.; Höglund-Isaksson, L.; Humpenöder, F.; Purohit, P.; Van Vuuren, D. Uncertainty in non-CO_2 greenhouse gas mitigation contributes to ambiguity in global climate policy feasibility. *Nat. Commun.* **2023**, *14*, 2949. [CrossRef]
5. International Energy Agency. CO_2 Emissions in 2023. Available online: https://www.iea.org/reports/co2-emissions-in-2023 (accessed on 25 October 2024).
6. Campbell, C.; Zentner, R.; Liang, B.C.; Roloff, G.; Gregorich, E.; Blomert, B. Organic C accumulation in soil over 30 years in semiarid southwestern Saskatchewan–effect of crop rotations and fertilizers. *Can. J. Soil Sci.* **2000**, *80*, 179–192. [CrossRef]
7. Lambin, E.F.; Turner, B.L.; Geist, H.J.; Agbola, S.B.; Angelsen, A.; Bruce, J.W.; Coomes, O.T.; Dirzo, R.; Fischer, G.; Folke, C.; et al. The causes of land-use and land-cover change: Moving beyond the myths. *Glob. Environ. Chang.* **2001**, *11*, 261–269. [CrossRef]
8. Houghton, R.; Hackler, J. Sources and sinks of carbon from land-use change in China. *Glob. Biogeochem. Cycles* **2003**, *17*, 1034. [CrossRef]
9. Houghton, R.A. The annual net flux of carbon to the atmosphere from changes in land use 1850–1990. *Tellus B Chem. Phys. Meteorol.* **1999**, *51*, 298–313. [CrossRef]
10. Houghton, R.A.; House, J.I.; Pongratz, J.; Van Der Werf, G.R.; Defries, R.S.; Hansen, M.C.; Le Quéré, C.; Ramankutty, N. Carbon emissions from land use and land-cover change. *Biogeosciences* **2012**, *9*, 5125–5142. [CrossRef]
11. Li, X.; Wang, X.; Hua, H. Research on influences of land use structure change on carbon emissions. *Ecol. Econ.* **2018**, *34*, 14–19.
12. Hung, L.Q.; Asaeda, T.; Thao, V.T.P. Carbon emissions in the field of land use, land use change, and forestry in the Vietnam mainland. *Wetl. Ecol. Manag.* **2021**, *29*, 315–329. [CrossRef]
13. Zhang, P.; He, J.; Hong, X.; Zhang, W.; Qin, C.; Pang, B.; Li, Y.; Liu, Y. Carbon sources/sinks analysis of land use changes in China based on data envelopment analysis. *J. Clean. Prod.* **2018**, *204*, 702–711. [CrossRef]
14. Zheng, X.; Cheng, J.M.; Zheng, S. Research on carbon emissions and influence factors in Wuhu City based on the change of land use structure. *Res. Soil Water Conserv.* **2012**, *19*, 259–262.
15. Zhao, R.; Huang, X.; Liu, Y.; Zhong, T.; Ding, M.; Chuai, X. Carbon emission of regional land use and its decomposition analysis: Case study of Nanjing City, China. *Chin. Geogr. Sci.* **2015**, *25*, 198–212. [CrossRef]
16. Zhao, J.; Kou, L.; Wang, H.; He, X.; Xiong, Z.; Liu, C.; Cui, H. Carbon emission prediction model and analysis in the Yellow River basin based on a machine learning method. *Sustainability* **2022**, *14*, 6153. [CrossRef]
17. Yang, F.; He, F.; Li, S.; Li, M.; Wu, P. A new estimation of carbon emissions from land use and land cover change in China over the past 300 years. *Sci. Total Environ.* **2023**, *863*, 160963. [CrossRef]
18. Jin, Y.; Sharifi, A.; Li, Z.; Chen, S.; Zeng, S.; Zhao, S. Carbon emission prediction models: A review. *Sci. Total Environ.* **2024**, *927*, 172319. [CrossRef]
19. Yue, T.; Long, R.; Chen, H.; Zhao, X. The optimal CO_2 emissions reduction path in Jiangsu province: An expanded IPAT approach. *Appl. Energy* **2013**, *112*, 1510–1517. [CrossRef]
20. Wang, Y.G.; Wang, X.; Sun, C.H.; Lu, X.Y. Research progress on the application of IPAT model and its variants. *Chin. J. Appl. Ecol.* **2015**, *26*, 949–957. [CrossRef]
21. Fang, K.; Tang, Y.; Zhang, Q.; Song, J.; Wen, Q.; Sun, H.; Ji, C.; Xu, A. Will China peak its energy-related carbon emissions by 2030? Lessons from 30 Chinese provinces. *Appl. Energy* **2019**, *255*, 113852. [CrossRef]
22. Zhang, P.; He, J.; Hong, X.; Zhang, W.; Qin, C.; Pang, B.; Li, Y.; Liu, Y. Regional-level carbon emissions modelling and scenario analysis: A STIRPAT case study in Henan province, China. *Sustainability* **2017**, *9*, 2342. [CrossRef]
23. Su, K.; Lee, C.M. When will China achieve its carbon emission peak? A scenario analysis based on optimal control and the STIRPAT model. *Ecol. Indic.* **2020**, *112*, 106138. [CrossRef]
24. Ye, C.; Ming, T. Land use carbon emissions estimation and carbon emissions control strategy effect scenario simulation in Zhejiang province. *Heliyon* **2023**, *9*, e20783. [CrossRef] [PubMed]
25. Li, F.; Xu, Z.; Ma, H. Can China achieve its CO_2 emissions peak by 2030? *Ecol. Indic.* **2018**, *84*, 337–344. [CrossRef]
26. Yu, Y.; Xu, W. Impact of FDI and R&D on China's industrial CO_2 emissions reduction and trend prediction. *Atmos. Pollut. Res.* **2019**, *10*, 1627–1635. [CrossRef]
27. Tong, X.; Chen, K.; Li, G. Influencing Factors Analysis and Trend Forecasting of China's Carbon Emissions—Empirical Study Based on STIRPAT and GM(1,1) Models. *J. Northeast. Univ. Nat. Sci.* **2015**, *36*, 297–300. [CrossRef]
28. Li, Y.; Wei, Y.; Dong, Z. Will China achieve its ambitious goal?—Forecasting the CO_2 emission intensity of China towards 2030. *Energies* **2020**, *13*, 2924. [CrossRef]

29. Malik, A.; Hussain, E.; Baig, S.; Khokhar, M.F. Forecasting CO_2 emissions from energy consumption in Pakistan under different scenarios: The China–Pakistan economic corridor. *Greenh. Gases Sci. Technol.* **2020**, *10*, 380–389. [CrossRef]
30. Huang, Y.; Shen, L.; Liu, H. Grey relational analysis, principal component analysis and forecasting of carbon emissions based on long short-term memory in China. *J. Clean. Prod.* **2019**, *209*, 415–423. [CrossRef]
31. He, X.; Song, Y.; Yu, F.; Duan, H. Applications of fractional order logistic grey models for carbon emission forecasting. *Fractal Fract.* **2024**, *8*, 145. [CrossRef]
32. Wang, L.; Xue, W. A study of the pathway to peak carbon in China. *Environ. Prot. Eng.* **2024**, *50*, 71–89. [CrossRef]
33. Cui, L.B.; Li, X.; Duan, H.B. Synergistic effects of reducing pollution and carbon emissions in the Yangtze River Delta. *China Popul. Resour. Environ.* **2024**, *34*, 21–32. [CrossRef]
34. National Development and Reform Commission. Yangtze River Delta Integration Development Index Report. 2022. Available online: https://www.ndrc.gov.cn/xwdt/ztzl/cjsjyth1/xwzx/202212/t20221229_1344571.html (accessed on 15 October 2024).
35. The State Council. State Council on the Issuance of the 13th Five-Year Plan Notification of the Work Programme for Controlling Greenhouse Gas Emissions. Available online: https://www.gov.cn/zhengce/content/2016-11/04/content_5128619.htm (accessed on 25 October 2024).
36. Yang, J.; Huang, X. 30 m annual land cover and its dynamics in China from 1990 to 2019. *Earth Syst. Sci. Data* **2021**, *13*, 3907–3925. [CrossRef]
37. Fang, J.; Guo, Z.; Piao, S.; Chen, A. Terrestrial vegetation carbon sinks in China, 1981–2000. *Sci. China D Earth Sci.* **2007**, *50*, 1341–1350. [CrossRef]
38. Lin, Q.; Zhang, L.; Qiu, B.; Zhao, Y.; Wei, C. Spatiotemporal analysis of land use patterns on carbon emissions in China. *Land* **2021**, *10*, 141. [CrossRef]
39. Strassmann, K.; Joos, F.; Fischer, G. Simulating effects of land use changes on carbon fluxes: Past contributions to atmospheric CO_2 increases and future commitments due to losses of terrestrial sink capacity. *Tellus B Chem. Phys. Meteorol.* **2008**, *60*, 583–603. [CrossRef]
40. Yang, Y.; Shi, Y.; Sun, W.; Chang, J.; Zhu, J.; Chen, L.; Wang, X.; Guo, Y.; Zhang, H.; Yu, L.; et al. Terrestrial carbon sinks in China and around the world and their contribution to carbon neutrality. *Sci. China Life Sci.* **2022**, *65*, 861–895. [CrossRef]
41. Zhou, Y.; Chen, M.; Tang, Z.; Mei, Z. Urbanization, land use change, and carbon emissions: Quantitative assessments for city-level carbon emissions in Beijing-Tianjin-Hebei region. *Sustain. Cities Soc.* **2021**, *66*, 102701. [CrossRef]
42. Fan, J.; Yu, X.; Zhou, L. Carbon emission efficiency growth of land use structure and its spatial correlation: A case study of Nanjing City. *Geogr. Res.* **2018**, *37*, 2177–2192. [CrossRef]
43. Yuan, S.F.; Tang, Y.Y. Spatial differentiation of land use carbon emission in the Yangtze River economic belt based on low carbon perspective. *Econ. Geogr.* **2019**, *39*, 190–198. [CrossRef]
44. Huang, H.; Zhou, J. Study on the spatial and temporal differentiation pattern of carbon emission and carbon compensation in China's provincial areas. *Sustainability* **2022**, *14*, 7627. [CrossRef]
45. Rong, T.; Zhang, P.; Zhu, H.; Jiang, L.; Li, Y.; Liu, Z. Spatial correlation evolution and prediction scenario of land use carbon emissions in China. *Ecol. Inf.* **2022**, *71*, 101802. [CrossRef]
46. Zhang, Z.Q.; Lao, Y.L.; Zhao, N.J.; Wei, J.H.; Hu, B.Q. Decoupling Relationship of Landuse Carbon Emission Reduction and Economic Growth in Guangdong Province. *Bull. Soil Water Conserv.* **2022**, *42*, 250–258, 266. [CrossRef]
47. Zhang, Y.; Dai, Y.; Chen, Y.; Ke, X. The study on spatial correlation of recessive land use transformation and land use carbon emission. *China Land Sci.* **2022**, *36*, 100–112. [CrossRef]
48. York, R.; Rosa, E.A.; Dietz, T. STIRPAT, IPAT and ImPACT: Analytic tools for unpacking the driving forces of environmental impacts. *Ecol. Econ.* **2003**, *46*, 351–365. [CrossRef]
49. Ehrlich, P.R.; Holdren, J.P. Impact of Population Growth: Complacency concerning this component of man's predicament is unjustified and counterproductive. *Science* **1971**, *171*, 1212–1217. [CrossRef]
50. Dietz, T.; Rosa, E.A. Rethinking the environmental impacts of population, affluence and technology. *Hum. Ecol. Rev.* **1994**, *1*, 277–300.
51. Zou, X.Q.; Sun, X.C.; Ge, T.Y.; Xing, S. Carbon emission differences, influence mechanisms and carbon peak projections in Yangtze river delta region. *Resour. Environ. Yangtze Basin* **2023**, *32*, 548–557. [CrossRef]
52. Zhou, J.; Yang, L.; Dong, M.N.; Jiang, L.L.; Wang, Y.; Zang, S.Y. Carbon Emissions Intensity Change Analysis Based on Land Use in Harbin City from 2004 to 2012. *Sci. Geogr. Sin.* **2015**, *35*, 322–327. [CrossRef]
53. Zhao, R.Q.; Huang, X.J.; Chuai, X.W. Misunderstandings and Future Trends of Researches on Land Use Carbon Emissions in China. *China Land Sci.* **2016**, *30*, 83–92. [CrossRef]
54. Lv, T.; Hu, H.; Zhang, X.; Wang, L.; Fu, S. Impact of multidimensional urbanization on carbon emissions in an ecological civilization experimental area of China. *Phys. Chem. Earth* **2022**, *126*, 103120. [CrossRef]
55. Chen, Y.Q. Prediction of Peak Carbon Emissions in Jiangsu Province Based on STIRPAT Model. Master's Thesis, Nanjing Forestry University, Nanjing, China, 2017.
56. Li, X.J.; Zhu, Q.X.; Qi, Z.Q.; Wang, T.B.; Zhang, Y.J. Prediction of carbon emission peak based on STIRPAT model: A case study of Gansu Province. *Environ. Prot. Technol.* **2022**, *28*, 38–44. [CrossRef]
57. Sun, L.L.; Cui, H.J.; Ge, Q.S. Will China achieve its 2060 carbon neutral commitment from the provincial perspective? *Adv. Clim. Chang. Res.* **2022**, *13*, 169–178. [CrossRef]

58. Liu, D.; Xiao, B. Can China achieve its carbon emission peaking? A scenario analysis based on STIRPAT and system dynamics model. *Ecol. Indic.* **2018**, *93*, 647–657. [CrossRef]
59. Jiang, H.Q.; Li, Y.X.; Chen, M.M.; Shao, X.X. Prediction and Realization Strategy of the Carbon Peak of the Industrial Sector in Zhejiang Province under the Vision of Carbon Neutrality. *Areal Res. Dev.* **2022**, *41*, 157–161, 168. [CrossRef]
60. Qin, L. Research on Influencing Factors and Prediction of Land Use Carbon Emissions in Jiangsu Province. Master's Thesis, China University of Mining and Technology, Xuzhou, China, 2022.
61. Wang, C.; Cai, W.J. China Provincial and High Spatial Accuracy Population Change Scenario Dataset (2010–2100). Available online: https://bbs.pinggu.org/thread-11382030-1-1.html (accessed on 25 October 2024).
62. Jiang, T.; Zhao, J.; Cao, L.G.; Wang, Y.J.; Su, B.D.; Jing, C.; Wang, R.; Gao, C. Projection of national and provincial economy under the shared socioeconomic pathways in China. *Adv. Clim. Chang. Res.* **2018**, *14*, 50–58. [CrossRef]
63. Pan, D.; Li, N.; Li, F.; Feng, K.S.; Peng, L.L.; Wang, Z. Mitigation strategy of Eastern China based on energy-source carbon emission estimation. *J. Environ. Sci.* **2021**, *41*, 1142–1152. [CrossRef]
64. Lin, B.Q.; Liu, X.Y. China's Carbon Dioxide Emissions under the Urbanization Process: Influence Factors and Abatement Policies. *Econ. Res. J.* **2010**, *45*, 66–78.
65. Wang, S.J.; Mo, H.B.; Fang, C.L. Carbon emissions dynamic simulation and its peak of cities in the Pearl River Delta Urban Agglomeration. *Chin. Sci. Bull.* **2022**, *67*, 670–684. [CrossRef]
66. Institute of Resources and Environmental Policy, Development Research Center of The State Council. China Energy Revolution Progress Report. 2020. Available online: https://www.coalchina.org.cn/uploadfile/2020/1109/20201109092028882.pdf (accessed on 25 October 2024).
67. China National Petroleum Corporation. World and China Energy Outlook 2050. Available online: https://m.in-en.com/article/html/energy-2255134.shtml (accessed on 25 October 2024).
68. Gu, W.W. Research on Policy Termination and Policy Renewal: A Case Study of the Policy of Returning Farmland to Forest. Master's Thesis, Capital University of Economics and Business, Beijing, China, 2011.
69. Dai, D.; Zhang, L.; Zhao, S.; Zhou, B. Forecast of carbon emission peak in Anhui Province under environmental regulation. *Fresenius Environ. Bull.* **2022**, *31*, 11202–11211.
70. Li, J.B.; Huang, X.J.; Chuai, X.W.; Sun, S.C. Scenario Simulation of Carbon Emissions in the Yangtze River Delta under the Background of "Dual Carbon". *Ecol. Econ.* **2022**, *38*, 13–18, 35.
71. Cui, Y.F. Research on the Characteristics and Influencing Factors of Land Use Carbon Emissions in the Yangtze River Delta Urban Agglomeration. Master's Thesis, China University of Mining and Technology, Xuzhou, China, 2019.